Journal of the Serbian Chemical Society
JSCS-info@shd.org.rs • www.shd.org.rs/JSCS
J. Serb. Chem. Soc. *79* (3) 361–377 (2014) UDC 628.3+535.6–26:544.4:66.011:66.099.72
JSCS–4591 *Original scientific paper*

Kinetics and optimization of the decoloration of dyeing wastewater by a schorl-catalyzed Fenton-like reaction

HUAN-YAN XU*, WEI-CHAO LIU, SHU-YAN QI, YAN LI, YUAN ZHAO and JI-WEI LI

School of Material Science and Engineering, Harbin University of Science and Technology, Harbin, 150040, P. R. China

(Received 25 February, revised 17 June 2013)

Abstract: The kinetics and optimization of the decoloration of an active commercial dye, argazol blue BFBR (ABB), by a heterogeneous Fenton-like reaction catalyzed by natural schorl were investigated in this study. The kinetic investigations revealed that the first-order kinetic model was more favorable to describe the decoloration of ABB under different reaction conditions than the second-order and Behnajady–Modirshahla–Ghanbery models. The relationship between the reaction rate constant k and reaction temperature T followed the Arrhenius Equation, with an apparent activation energy E_a of 51.31 kJ·mol^{-1}. The central composite design under the response surface methodology was employed for the experimental design and optimization of the ABB decoloration process. The significance of a second order polynomial model for predicting the optimal values of ABB decoloration was evaluated by the analysis of variance and 3D response surface plots for the interactions between the two variables were constructed. Then, the optimum conditions were determined.

Keywords: schorl; heterogeneous catalysis; argazol blue BFBR; response surface methodology; first-order kinetics.

INTRODUCTION

Different dyes can be found in effluents from various industries, such as the food processing, cosmetics, paper and pulp, dye manufacture, printing and textile industries.[1] Effluent containing reactive dyes from textile dyeing and finishing industries is a significant source of environmental pollution. Reactive dyes are extensively used to color cellulose and rayon textiles due to their bright colors, excellent colorfastness and easy dyeing operations. About 45 % of the annual production (700,000 tons) of commercially available dyestuffs belongs to the reactive dye class. Up to 50 % of a reactive dye can be hydrolyzed and left unusable in the dye bath. Reactive dyes are resistant to decomposition due to their aromatic molecular structures, and thus can remain in the environment for a

* Corresponding author. E-mail: xhy7587@aliyun.com
doi: 10.2298/JSC130225075X

long time.[2] With the increasing concern about environment protection, removal of dyes from wastewater has become a significant issue.[3] The discharge of dye wastewater into the environment induces both toxicological and esthetical problems as it can impede light, damage water resources and make food-chain organisms toxic.[4] Various treatment methods, such as sedimentation, chemical coagulation, electrochemical methodology, and biological treatment, have been extensively investigated. However, most of the above methods suffer from one or more limitations and none of them were successful in the complete removal of color from wastewater.[5] As one important kind of reactive dyes, the Argazol® BF series have a vinyl sulfone and a monochlorotriazine group, and show low sensitivity to variations in the following dyeing parameters, liquor ratio, dyeing temperature, salt, alkali, dyeing time, *etc*. Thus, Argazol® BF reactive dyes have been widely used for piece dyeing, package yarn dyeing, hank yarn dyeing, jigger dyeing and continuous dyeing. To the best of our knowledge, scarce reports have been published on the treatment of wastewater containing Argazol® BF reactive dyes.

In the last decades, advanced oxidation processes (AOPs) appeared to be an effective method for the degradation of refractory organic contaminants in waters and soils.[6–9] AOPs involves the *in situ* generation of hydroxyl radical ($^{\bullet}OH$), achieving the complete conversion of the target pollutant species to CO_2, H_2O and mineral acids,[10] *i.e.*, mineralization. Among all AOPs, the Fenton reaction, employing hydrogen peroxide (H_2O_2) as oxidant and ferrous ion as catalyst, has been regarded as one of the most powerful and attractive ones available.[6] However, for classic Fenton reagent, there were a number of disadvantages such as narrow pH range and Fe ions as secondary pollutants.[11] In principle, these limitations could be overcome by using heterogeneous Fenton-type catalysts, instead of homogeneous iron ions.

It is well accepted that the most important issue in a heterogeneous Fenton process was the development of a heterogeneous catalyst with high catalytic activity and long-term stability at a reasonable cost.[12] Low-cost mineral materials with special crystal structures or properties were the best alternatives as heterogeneous Fenton catalysts, behaving as the iron supporter or promoter. This process is called a mineral-catalyzed Fenton-like system. Natural iron-bearing minerals could be employed as iron sources to promote the generation of $^{\bullet}OH$ from H_2O_2. The main advantages of the application of iron minerals in Fenton chemistry are as follows: a) periods of catalyst life could be extended without the need for regeneration or replacement; b) the catalyst could be removed from the treated water by sedimentation or filtration; c) the pH of the treated media could be in the range 5–9; d) the reaction was almost insensitive to the concentration of inorganic carbonate.[13] However, in some cases, the degradation rates of organic substrates in these Fenton-like systems seemed to be slow. To accelerate the

degradation rate, ultrasonic or UV irradiation was often applied to assist Fenton-like systems.[14,15] Otherwise, an electrostatic field could also enhance the mineral-catalyzed Fenton-like system.[16,17] Schorl is one kind of minerals of the tourmaline group, which are complex borosilicate minerals belonging to the trigonal space group R3m.[18] The general formula of tourmaline can be written as $XY_3Z_6[T_6O_{18}][BO_3]V_3W$, where X = Ca, Na, K; Y = Li, Mg, Fe^{2+}, Mn^{2+}, Al, Cr^{3+}, V^{3+}, Fe^{3+}, (Ti^{4+}); Z = Mg, Al, Fe^{3+}, V^{3+}, Cr^{3+}; T = Si, Al; B=B; V = OH, O; W = OH, F, O.[19] The basic structural units are hexagonal rings of Si_6O_{18} that form the basal plane and are connected with Na, Li and Al octahedra and distorted BO_3 groups in planar coordination along [0001] with a three-fold symmetry structure.[20] Depending on the occupancy of the Y and X sites, tourmalines are classified as end members, dravite (Y = Mg), schorl (Y = Fe^{2+}), tsilaisite (Y = Mn), olenite (Y = Al) and elbaite (Y = Li, Al).[21] Due to the special crystal structure of a tourmaline, spontaneous “electrostatic poles” exist on its surface.[22] Thus, schorl is not only a natural iron-bearing mineral, but also has unique characteristics of pyroelectricity and piezoelectricity.

Encouraged by this, a Fenton-like reaction catalyzed by natural schorl was investigated for the degradation of various organic substrates.[23–25] These results revealed the schorl-catalyzed Fenton-like reaction could be effective for the decoloration of dyeing wastewater and the electrostatic field on the surface of schorl crystal could enhance the decoloration process. Nevertheless, the kinetics and optimization of this reaction process were not studied further, which could be beneficial to the engineering aspects of the process. Hence, the present study focused on the optimization of the decoloration of a commercial dye, argazol blue BFBR (ABB), by the schorl-catalyzed Fenton-like reaction using the response surface methodology (RSM). Meanwhile, the kinetic process is discussed in details, involving the comparison of three kinetic models.

EXPERIMENTAL

Materials

Powdered particles of schorl, in the size range of < 64 μm, were purchased from Wuhua-Tianbao Mining Resources Co. Ltd., Inner Mongolia, China. The particles of the natural sample were directly used in the experimental studies without any treatment. The schorl samples were characterized by X-ray diffraction (XRD) analysis, Fourier transform infrared spectroscopy (FTIR) and scanning electron microscopy (SEM) with X-ray energy dispersive spectroscopy (EDS). Detailed information, including equipment, conditions, procedures and respective characterization data, were described elsewhere.[25] All chemical reagents used in this study were of analytical grade. Solutions were prepared in deionized water.

Decoloration methods

A stock solution containing ABB (2000 $mg \cdot L^{-1}$) was prepared and subsequently diluted to the required concentrations for the experimental work. The pH was adjusted by addition of sodium hydroxide (NaOH) and nitric acid (HNO_3) to the ABB solutions. The concentration of hydrogen peroxide (H_2O_2) was 30 %. Then, the schorl sample was added into 100 mL of solu-

tion of the required concentration of ABB in a conical flask. After sealing, the conical flasks were placed in a constant-temperature water-bath at different temperatures for different contact times. At regular time intervals, 2 mL of the reaction solution was collected from the reactor for measurements of the ABB concentration, using a 721-type UV–Vis spectrophotometer at a wavelength of 608 nm. The residual ratio, c_t/c_0, was used to express the decoloration efficiency of ABB, where c_0 is the initial concentration of the ABB wastewater and c_t the concentration at contact time t. In order to check the reproducibility of the results, random tests were performed for different experimental conditions.

Kinetic models

The kinetics of Fenton process can be quite complex owing to the large number of steps realized simultaneously during the process. Three kinetic models, the first-order, the second-order and Behnajady–Modirshahla–Ghanbery (BMG), were employed to test the fitting of experimental data obtained from the decoloration processes. The linear forms of these models are given in Eqs. (1)–(3), respectively:[26]

$$\ln\frac{c_0}{c_t} = k_1 t \tag{1}$$

$$\frac{1}{c_t} - \frac{1}{c_0} = k_2 t \tag{2}$$

$$\frac{t}{1-(c_t/c_0)} = m + bt \tag{3}$$

where k_2 is the second-order rate constant, and m and b are the two constants of the BMG model relating to oxidation capacities and reaction kinetics. The reaction rate constants for the heterogeneous Fenton decoloration of ABB were gained using linear regression of the three models. The order of the reaction was determined by the quantity of linear fit *via* the coefficient of determination (R^2).[27]

Experimental design, analysis and optimization

Central composite design (CCD) under the response surface methodology (RSM) was employed for the experimental design and optimization of ABB decoloration process. Base on previous experience of dyeing wastewater treatment in industrial applications, four factors, in this work, were selected as independent variables. They are the H_2O_2 concentration (mM), the schorl dosage ($g \cdot L^{-1}$), the solution pH and the reaction time (min), assigned with the following notations X_1, X_2, X_3 and X_4, respectively. The decoloration ratio of ABB (Y, %) was chosen as the output variable (response). Since the typical temperature of wastewater drained from dyeing and finishing mills is usually around 50 °C,[28] the temperature of the ABB simulated wastewater was maintained at 50 °C for all the designed experiments. The experimental design, mathematical modeling and optimization were performed with Design Expert 8.0.5.0 software (Stat-Ease, Inc.). For the statistical calculations, the variable X_i was coded as x_i according to the following equation:[29]

$$x_i = \frac{X_i - X_0}{\delta X} \tag{4}$$

where x_i is the code value, X_i is the uncoded value, X_0 is the value of X_i at the center point and δX presents the step change. The experimental ranges and the levels of the independent variables for ABB decoloration are listed in Table I. Preliminary experiments were imple-

mented to determine the ranges of the independent variables. A second-order regression model was employed to analyze and fit the responses to the independent variables (Eq. (5)):[30,31]

$$Y = \beta_0 + \sum_{i=1}^{k} \beta_i X_i + \sum_{i=1}^{k} \beta_{ii} X_i^2 + \sum_i \sum_j \beta_{ij} X_i X_j \quad (5)$$

where Y is response (ABB decoloration ratio); X_i and X_j input variables that influence the response (Y); β_0 an intercept constant; β_i the first-order regression coefficient; β_{ii} the second--order regression coefficient representing the quadratic effect of factor i; and β_{ij} the coefficient of interaction between factors i and j. Analysis of variance (ANOVA) was conducted to determine the significance of the model and the regression coefficient. Otherwise, it should be mentioned that all experiments were performed in duplicate and the average of the decoloration ratio was taken as the response. The standard deviation (*SD*) was less than 3 %.[32]

TABLE I. Variables and their codes and real experimental values used in the CCD

Variable	Coded level				
	–2	–1	0	1	2
X_1 / mM	0	9.69	19.38	29.07	38.76
X_2 / g·L^{-1}	0	2.5	5	7.5	10
X_3	2	4	6	8	10
X_4 / min	0	5	10	15	20

RESULTS AND DISCUSSION

Decoloration of ABB

A series of experimental results demonstrated that the ABB decoloration efficiency increased by, respectively, increasing the H_2O_2 concentration, the schorl dosage, temperature and by decreasing the pH. Figure 1 clearly indicates that the ABB decoloration efficiency increases with increasing H_2O_2 concentration. When the added H_2O_2 concentration was 9.69 mM, , about half of the

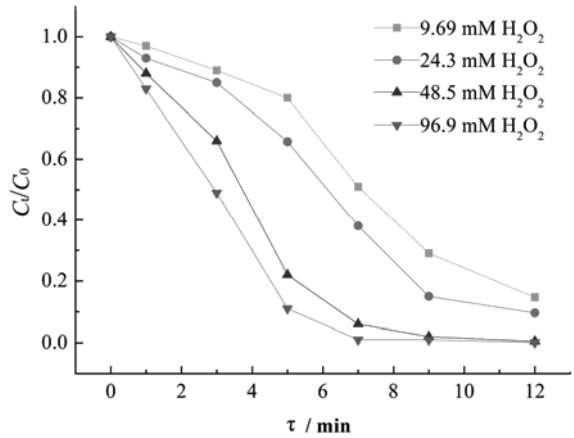

Fig. 1. The effect of H_2O_2 concentration on ABB decoloration by the schorl-catalyzed Fenton-like reaction at pH 6, T = 328 K, $[ABB]_0$ = 200 mg·L^{-1} and $[schorl]_0$ = 10 g·L^{-1}.

ABB dye had been decolored after 7 min of reaction; whereas it was completely decolored within the same reaction time when the concentration of added H_2O_2 was 96.9 mM. The increase in the H_2O_2 concentration resulted in an increase in the reaction activity, as expected, due to an increase of $^{\bullet}OH$.[33] It should be noted that the ABB decoloration efficiency increased most significantly when H_2O_2 concentration was increased from 24.3 to 48.5 mM. For a higher addition of H_2O_2, the decoloration efficiency increased slowly because of the scavenging of $^{\bullet}OH$ by the excess H_2O_2.[34]

The effect of schorl dosage on the decoloration efficiency of ABB was also investigated in this work. The results presented in Fig. 2 show that the activity of this heterogeneous Fenton system for ABB decoloration increases with increasing schorl dosage. This behavior could be attributed to the fact that with increasing amount of schorl catalyst, more active Fe sites are available on the catalyst surface for accelerating the decomposition of H_2O_2 (heterogeneous catalysis), and more Fe ion are leached into the solution, leading to an increase in the number of $^{\bullet}OH$ radicals (homogeneous catalysis).[25] Similar results were observed in Fenton-like reactions catalyzed by other Fe-bearing minerals.[35,36]

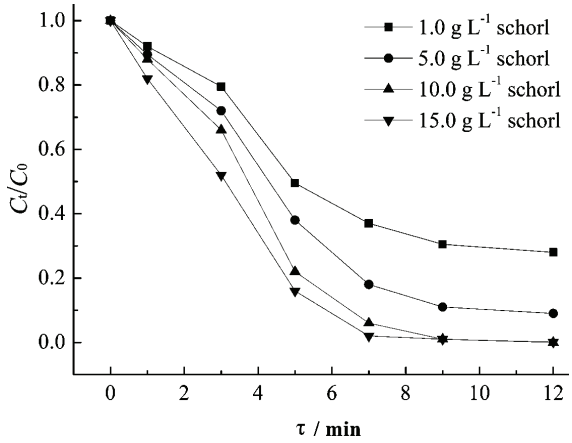

Fig. 2. The effect of the schorl dosage on ABB decoloration by schorl-catalyzed Fenton-like reaction at pH 6, T = 328 K, $[ABB]_0$ = 200 mg·L^{-1} and $[H_2O_2]_0$ = 48.5 mM.

The typical temperature of the textile effluents was usually around 50 °C.[28] Therefore, a temperature range of 25–65 °C (corresponding to 298–338 K) was studied with the goal of investigating the effect of this parameter on ABB decoloration. The results are shown in Fig. 3, from which it could be observed that the decoloration efficiency increased with increasing reaction temperature. A possible reason for this phenomenon might be that higher temperatures could provide more energy for the reactant molecules to overcome the reaction activation energy; hence, resulting in faster dye decoloration.[37] Another interpreta-

tion might be that increasing the reaction temperature accelerated the rate of •OH formation in the heterogeneous Fenton-like system.[33]

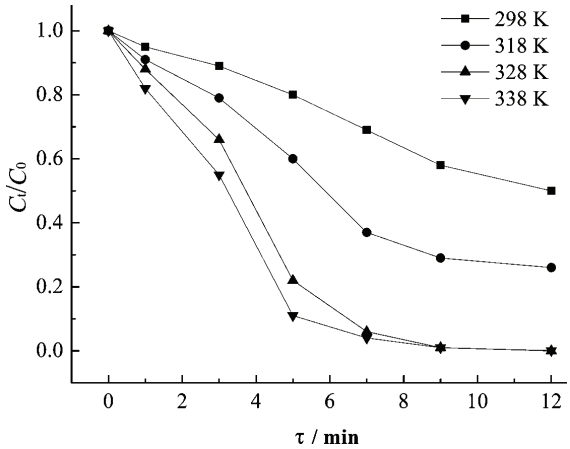

Fig. 3. The effect of reaction temperature on ABB decoloration by the schorl-catalyzed Fenton-like reaction at pH 6, $[ABB]_0$ = 200 mg·L^{-1}, $[H_2O_2]_0$ = 48.5 mM and $[schorl]_0$ = 10 g·L^{-1}.

Figure 4 suggests that, under the adopted experimental conditions, the reactivity of the system is dependent on the pH of the dye solution, exhibiting different decoloration behavior at acidic and alkaline pH values. At acidic pH values (2 and 4), more Fe ions were dissolved from the schorl catalyst into the solution, which then catalyzed the generation of more •OH from H_2O_2, resulting in a faster decoloration of dye by homogeneous catalysis of the process. At neutral and

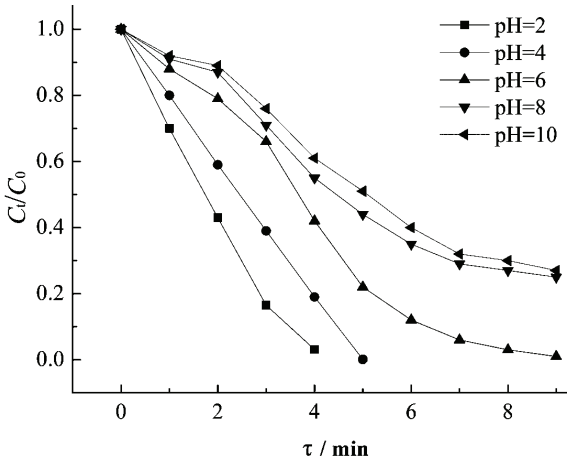

Fig. 4. The effect of solution pH on ABB decoloration by the schorl-catalyzed Fenton-like reaction at T =328 K, $[ABB]_0$ = 200 mg·L^{-1}, $[H_2O_2]_0$ = 48.5 mM and $[schorl]_0$ = 10 g·L^{-1}.

alkaline pH (6, 8 and 10), because there were fewer Fe ions leaching into the solution, it was proposed that H_2O_2 decomposition was catalyzed by active Fe sites on the surface of the schorl catalyst, *i.e.*, heterogeneous catalysis governed this process.[25]

According to the discussions above, it could be concluded that as the possible reaction mechanism of ABB decoloration, besides minor adsorption, the Fenton-like reaction was responsible for the whole decoloration process, including heterogeneous and homogeneous catalysis. Under acidic pH conditions, the homogeneous catalytic reaction played an important role in ABB decoloration and the generation of $^{\bullet}OH$ could be described as follows, where ≡Fe(II) and ≡Fe(III) represent the Fe(II) and Fe(III) species on the schorl surface, respectively:

$$\equiv \mathrm{Fe(II)} \xrightarrow{\mathrm{H^+}} \mathrm{Fe^{2+}_{(aq)}} \quad (6)$$

$$\equiv \mathrm{Fe(III)} \xrightarrow{\mathrm{H^+}} \mathrm{Fe^{3+}_{(aq)}} \quad (7)$$

$$\mathrm{Fe^{2+}_{(aq)} + H_2O_2 \rightarrow\ Fe^{3+}_{(aq)} + {}^{\bullet}OH + OH^-} \quad (8)$$

$$\mathrm{Fe^{3+}_{(aq)} + H_2O_2 \rightarrow\ Fe^{2+}_{(aq)} + {}^{\bullet}OOH + H^+} \quad (9)$$

At alkaline pH conditions, the heterogeneous catalytic reaction played an important role in ABB decoloration and the generation of •OH could be described as follows:

$$\equiv \mathrm{Fe(II) + H_2O_2 \rightarrow\ \equiv Fe(III) + {}^{\bullet}OH + OH^-} \quad (10)$$

$$\equiv \mathrm{Fe(III) + H_2O_2 \rightarrow\ \equiv Fe(II) + {}^{\bullet}OOH + H^+} \quad (11)$$

Kinetic studies

The parameters of kinetic models for the decoloration of ABB by the schorl--catalyzed Fenton-like system under different reaction conditions were calculated by application of linear regression analysis to ln (c_0/c_t) *vs*. *t* data for the first-order model, [($1/c_t$)–($1/c_0$)] *vs*. *t* data for the second-order model and $t/[1-(c_t/c_0)]$ *vs*. *t* data for the BMG model. The obtained parameters are given in Table II, from which it could be seen that the fittings of the second-order and the BMG models to the experimental data were not good as evidenced by the low determination coefficients. However, the values of determination coefficients for the first-order model were mostly higher than those of the second-order and the BMG models. Therefore, the first-order kinetic model is the best one to describe the decoloration of ABB under different reaction conditions by the schorl-catalyzed Fenton-like process. It has been reported that the fitting of the experimental kinetic data for the decoloration of dyes by a heterogeneous Fenton-like reaction catalyzed by other Fe-containing minerals was good with the first-order model,

TABLE II. Kinetic parameters of three models and their determination coefficient (R^2) for ABB decoloration under different reaction conditions

$[ABB]_0$ mg·L^{-1}	$[H_2O_2]_0$ mM	$[schorl]_0$ g·L^{-1}	T K	pH	First-order		Second-order		Behnajady–Modirshahla–Ghanbery		
					k_1 / min^{-1}	R^2	k_2 / M^{-1}·min^{-1}	R^2	m / min	b	R^2
200	9.69	10	328	6	0.17896	0.91072	0.00252	0.76646	33.14958	–1.95302	0.79215
200	24.3	10	328	6	0.22854	0.92092	0.00438	0.81464	16.85968	–0.46215	0.13555
200	48.5	10	328	6	0.50218	0.97941	0.0808	0.62077	6.8709	0.29817	0.79136
200	96.9	10	328	6	0.62983	0.95648	0.38206	0.51113	4.0723	0.57088	0.7856
200	48.5	1	328	6	0.11927	0.90732	0.00126	0.95065	11.38154	0.25604	0.02569
200	48.5	5	328	6	0.23489	0.9386	0.00507	0.93071	8.48622	0.24922	0.12377
200	48.5	15	328	6	0.63549	0.97201	0.37971	0.48902	4.13205	0.57328	0.83566
200	48.5	10	298	6	0.06188	0.98094	0.00045	0.96262	23.32937	0.00826	0.2498
200	48.5	10	318	6	0.14822	0.93247	0.00141	0.93927	11.26378	0.27885	0.1532
200	48.5	10	338	6	0.62514	0.97894	0.37824	0.47713	4.232	0.56332	0.79455
200	48.5	10	328	2	1.03091	0.90636	0.04811	0.58126	1.77142	0.74711	0.93748
200	48.5	10	328	4	0.47267	0.94205	1.00053	0.33765	3.53286	0.50986	0.77193
200	48.5	10	328	8	0.19456	0.98036	0.00203	0.97207	11.60779	–0.17252	0.0815
200	48.5	10	328	10	0.17932	0.97706	0.0018	0.95966	14.10038	–0.42688	0.096

for instance, the decoloration of the azo dye Orange G catalyzed by goethite[38] and acid Orange II by natural vanadium–titanium magnetite.[39]

From Table II, it could also be seen that, for the first-order model, the reaction rate constant k increased with increasing H_2O_2 concentration, schorl dosage and reaction temperature, but decreased with increasing solution pH. Among them, the relationship between the rate constant k and reaction temperature T should be mentioned and discussed because of its complexity in all chemical reactions. The rate constant k increases when the reaction temperature increases, which suggested that the mobility of the reactants from the bulk medium to the heterogeneous surface and the converted products from the surface to the bulk medium were more favored by the applied thermal energy.[27] The relationship between k and T could be described by five different equations. In this study, it follows the Arrhenius equation, due to the linear relationship between ln k and $10^3/T$, as illustrated in Fig. 5. The apparent activation energy of ABB decoloration could be calculated by comparing the obtained fitting equation with Arrhenius Equation, shown as follows:[27]

$$\text{Fitting equation: } \ln k = \frac{6170.99}{T} + 17.8337 \tag{12}$$

$$\text{Arrhenius Equation: } \ln k = \frac{E_a}{RT} + \ln A \tag{13}$$

where E_a is the Arrhenius activation energy for the reaction process, indicating the minimum energy that the reactants must have for the reaction to proceed, A is the Arrhenius factor and R is the gas constant (8.314 J·mol^{-1}·K^{-1}). Thus, the apparent activation energy E_a of the reaction in this work was determined to be 51.31 kJ·mol^{-1}. Generally, the activation energy of an ordinary thermal reactions is between roughly 60 and 250 kJ·mol^{-1}.[38] In the present study, the obtained activation energy value of 51.31 kJ·mol^{-1} was lower than that of an ordinary

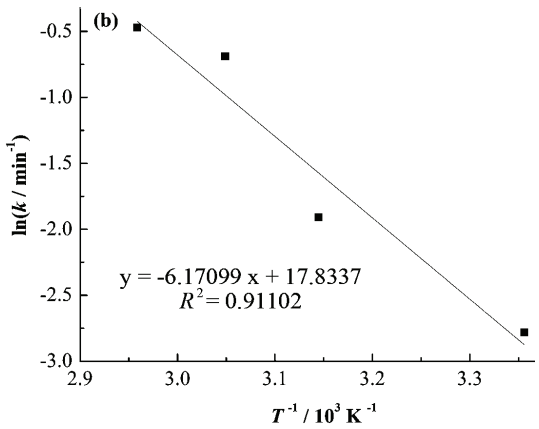

Fig. 5. The relationship between ln k and $10^3/T$.

thermal reaction, suggesting that this Fenton reaction process typically proceeds with a low energy barrier.[40]

Optimization by CDD under RSM

The effects of various experimental parameters (X_1, X_2, X_3 and X_4) in this reaction were investigated using CCD under RSM. Thirty experiments, with 4 factors and 5 levels for each factor were designed, which are listed in Table III. Among these 30 experiments, 6 experiments were repetition of the central point (run No. 1, 3, 17, 20, 21 and 24). All of the factors were in the centric point of their values in these experiments. The closeness of the responses of these 6 experiments could be a sign of the accuracy of the experiment process.[41] For predicting the optimal values of ABB decoloration within the experimental constrains, a second order polynomial model was fitted to the experimental results for the decoloration ratio of ABB. The obtained polynomial model is shown as follows:

$$\begin{aligned} Y = {} & 74.42 + 13.77X_1 + 4.45X_2 - 21.03X_3 + \\ & + 16.05X_4 + 0.40X_1X_2 - 4.81X_1X_3 - \\ & - 5.96X_1X_4 + 1.69X_2X_3 + 0.44X_2X_4 - \\ & - 3.00X_3X_4 - 6.00X_1^2 - 2.85X_2^2 - 2.93X_3^2 - 9.16X_4^2 \end{aligned} \quad (14)$$

TABLE III. Central composite design matrix together with the experimental and predicted values of the ABB decoloration ratios

Run	X_1 / mM	X_2 / g·L^{-1}	X_3	X_4 / min	Y / %	
					Experimental	Predicted
1	0.000	0.000	0.000	0.000	74.9	74.42
2	–1.000	–1.000	1.000	1.000	29.7	36.33
3	0.000	0.000	0.000	0.000	73.8	74.42
4	2.000	0.000	0.000	0.000	84.7	77.94
5	–1.000	1.000	–1.000	–1.000	24.8	32.83
6	0.000	2.000	0.000	0.000	79.7	71.91
7	–1.000	1.000	–1.000	1.000	91.3	83.73
8	–2.000	0.000	0.000	0.000	15.2	22.88
9	–1.000	1.000	1.000	1.000	43.5	48.68
10	1.000	1.000	–1.000	1.000	99.9	109.76
11	1.000	–1.000	1.000	1.000	49.6	41.51
12	0.000	0.000	0.000	–2.000	0.00	5.66
13	0.000	0.000	0.000	2.000	74.6	69.86
14	1.000	–1.000	–1.000	1.000	97.9	102.56
15	–1.000	–1.000	–1.000	1.000	85.3	78.13
16	0.000	–2.000	0.000	0.000	45.4	54.11
17	0.000	0.000	0.000	0.000	75.2	74.42
18	0.000	0.000	–2.000	0.000	99.8	104.76
19	0.000	0.000	2.000	0.000	24.7	20.66
20	0.000	0.000	0.000	0.000	73.8	74.42

TABLE III. Continued

Run	X_1 / mM	X_2 / g·L^{-1}	X_3	X_4 / min	Y / %	
					Experimental	Predicted
21	0.000	0.000	0.000	0.000	74.1	74.42
22	1.000	1.000	–1.000	–1.000	90.2	82.71
23	–1.000	1.000	1.000	–1.000	15.3	9.78
24	0.000	0.000	0.000	0.000	74.7	74.42
25	–1.000	–1.000	1.000	–1.000	9.10	–0.82
26	–1.000	–1.000	–1.000	–1.000	34.9	28.98
27	1.000	–1.000	1.000	–1.000	21.5	28.21
28	1.000	–1.000	–1.000	–1.000	82.5	77.26
29	1.000	1.000	1.000	1.000	50.4	55.46
30	1.000	1.000	1.000	–1.000	33.3	40.41

Statistical testing of this model was implemented by analysis of variance (ANOVA) and the results for the coded variable levels are given in Table IV. From the ANOVA analysis, it was shown that the calculated F value was 24.46, that is much larger than the critical value of 2.42 for $F_{0.05}$,[14,15] which implied that the derived quadratic polynomial model was significant.[42] The low probability value (p value < 0.0001) means that there was only a 0.01 % chance that such a model could occur due to noise.[32] The determination coefficient (R^2) quantitatively evaluated the correlation between the experimental data and the predicted responses.[29] The experimental results and the predicted ones obtained from the model (Eq. (8)) were compared and listed in Table III. It was found that

TABLE IV. ANOVA analysis for the obtained quadratic polynomial model

Source	Sum of squares	Degree of freedom	Mean square	F value	p-value (Prob>F)
Model	25921.02	14	1851.50	24.46	< 0.0001
X_1	4548.51	1	4548.51	60.09	< 0.0001
X_2	475.26	1	475.26	6.28	0.0242
X_3	10609.22	1	10609.22	140.15	< 0.0001
X_4	6182.46	1	6182.46	81.67	< 0.0001
X_1X_2	2.56	1	2.56	0.034	0.8566
X_1X_3	370.56	1	370.56	4.90	0.0429
X_1X_4	568.82	1	568.82	7.51	0.0152
X_2X_3	45.56	1	45.56	0.60	0.4499
X_2X_4	3.06	1	3.06	0.040	0.8433
X_3X_4	144.00	1	144.00	1.90	0.1880
X_1^2	988.11	1	988.11	13.05	0.0026
X_2^2	223.11	1	223.11	2.95	0.1066
X_3^2	235.00	1	235.00	3.10	0.0984
X_4^2	2303.71	1	2303.71	30.43	< 0.0001
Residual	1135.45	15	75.70	–	–
R^2			0.9580		
Adj. R^2			0.9189		
Pred. R^2			0.7586		

the predicted values matched the experimental ones reasonably well with R^2 = = 0.9580. Figure 6 (slope equals 1) suggests that the predicted decoloration ratio of ABB agrees well with the experimental values. Furthermore, the value of the adjusted determination coefficient (R^2) was also very high (0.9189), which indicated the high significance of the model.[27] In addition, values of Prob > F less than 0.0500 indicate that the model terms were significant and values greater than 0.1000 indicate that the model terms were not significant.[32] In this study, X_1, X_2, X_3, X_4, X_1X_3, X_1X_4, X_1^2, X_3^2 and X_4^2 were significant model terms. Thus, the statistical analysis of all experimental data showed that the H_2O_2 concentration, the schorl dosage, the solution pH and the reaction time had a significant effect on ABB decoloration in the schorl-catalyzed Fenton-like system.

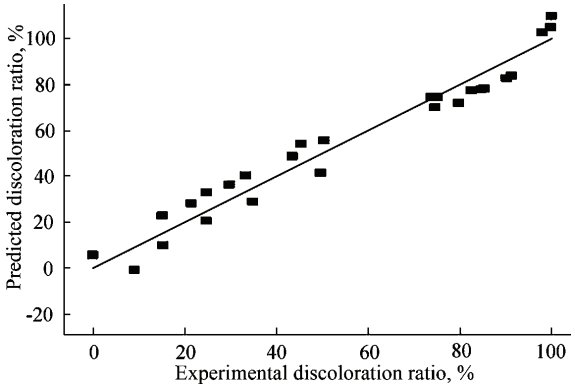

Fig. 6. Comparison of the predicted ABB decoloration ratios and the experimental values.

The 3D response surface plots for the interactions between two variables are presented in Fig. 7a–f with different interactions. As could be seen, the ABB decoloration ratio increased with increasing H_2O_2 concentration, schorl dosage and reaction time, but decreased with increasing solution pH, which is consistent with the one factorial experiment. The reasons have been interpreted in the section “Decoloration of ABB”. Nevertheless, the interactions between two independent variables were not significant, because the curvature of the three-dimensional surfaces was not pronounced.[31,43] The main goal of the optimization in this study was to determine the optimum values of the variables for the decoloration of ABB by the schorl-catalyzed Fenton-like reaction. Based on the model prediction, the optimum conditions for the decoloration of ABB by this process were determined to be 31.67 mM H_2O_2 concentration, 6.97 g·L^{-1} schorl dosage, solution pH 3.73 and 17.82 min reaction time, with the maximum ABB decoloration ratio of 99.94 %. The corresponding experimental value of ABB decoloration ratio under the optimum conditions was determined as 99.5 %, which was very close to the optimized one. It was confirmed that RSM was a powerful and satisfactory strategy to optimize the operational parameters of ABB decoloration by the heterogeneous Fenton-like reaction catalyzed by natural schorl.

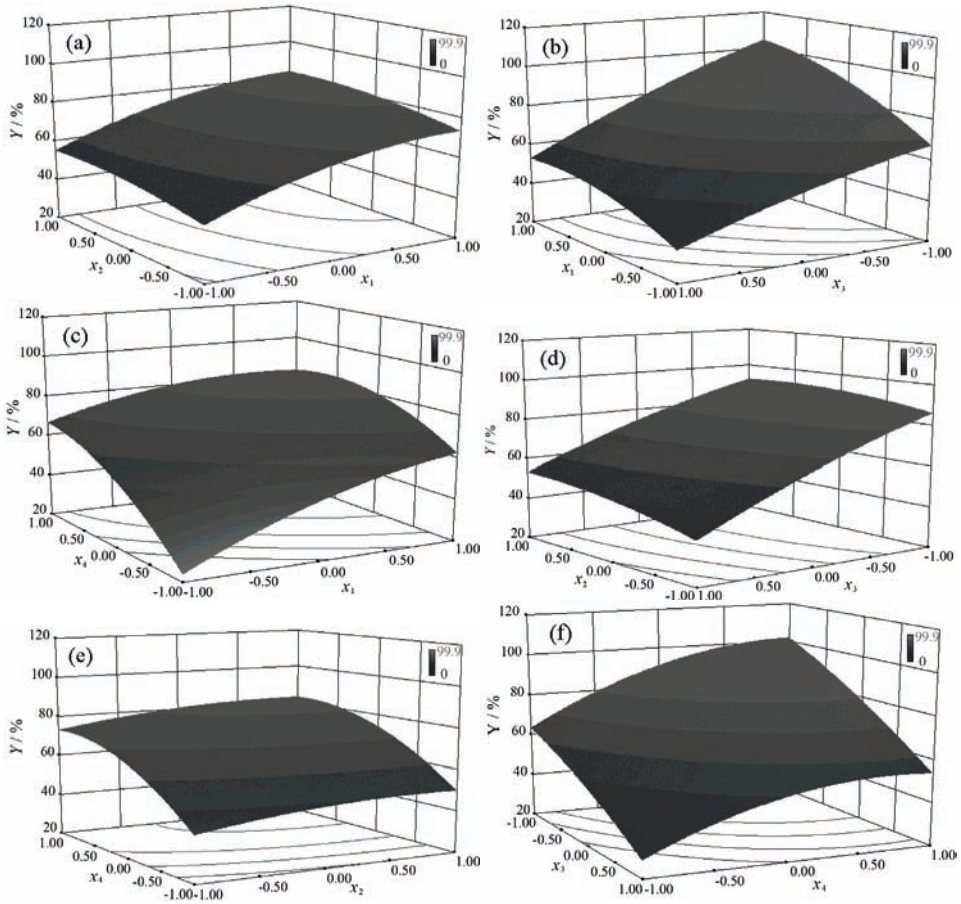

Fig. 7. The response surface plots for ABB decoloration with the interaction effect of: a) H_2O_2 concentration (X_1) and schorl dosage (X_2); b) H_2O_2 concentration (X_1) and solution pH (X_3); c) H_2O_2 concentration (X_1) and reaction time (X_4); d) schorl dosage (X_2) and solution pH (X_3); e) schorl dosage (X_2) and reaction time (X_4); f) solution pH (X_3) and reaction time (X_4).

CONCLUSIONS

The successful decoloration of dye ABB in water was achieved by the heterogeneous Fenton-like reaction using natural schorl as the catalyst. The efficiency of ABB decoloration increased with increasing H_2O_2 concentration, schorl dosage and reaction temperature, and decreasing solution pH. The first-order, second-order and BMG models were employed to investigate the kinetics of ABB decoloration. The values of determination coefficients for the first-order model were mostly higher than those of the second-order and BMG models. Therefore, first-order kinetic model was the best one to describe the decoloration of ABB under different reaction conditions. Further analysis indicated that the relationship between k and T followed the Arrhenius Equation, evidenced by the

linear relationship between ln k and $10^3/T$ and the apparent activation energy E_a of the reaction in this study was determined to be 51.31 kJ·mol^{-1}. CDD under RSM was used for the process optimization and 30 experiments, with 4 factors and 5 levels for each factor were designed. For predicting the optimal values of ABB decoloration within the experimental constrains, a second order polynomial model was fitted to the experimental results for the decoloration ratio of ABB. ANOVA analysis indicated the high significance of the model. 3D response surface plots for the interactions between two variables were constructed. Based on the model prediction, the optimum conditions for the decoloration of ABB by this process were determined to be 31.67 mM H_2O_2 concentration, 6.97 g·L^{-1} schorl dosage, solution pH 3.73 and 17.82 min reaction time, with the maximum ABB decoloration ratio of 99.94 %.

Acknowledgments. This work was supported by The National Natural Science Foundation of China (No. 51002040), The National College Students' Innovative Training Project (No. 201210214006) and The Science Foundation of the Heilongjiang Education Office (No. 12521071). Moreover, Prof. Huan-Yan Xu also expresses his appreciation for the financial support of the Program for New Century Excellent Talents in Heilongjiang Provincial Universities (No. 1253-NCET-010). Moreover, please add the following fund at the end of the part acknowledgements "Dr. Shu-Yan Qi shows her thank to Natural Science Youth Fund of Heilongjiang Province (No. QC2012C084).

ИЗВОД

КИНЕТИКА И ОПТИМИЗАЦИЈА ОБЕЗБОЈАВАЊА ОТПАДНЕ ВОДЕ ОД БОЈЕЊА ФЕНТОНСКОМ РЕАКЦИЈОМ КАТАЛИЗОВАНОМ ШОРЛОМ

HUAN-YAN XU, WEI-CHAO LIU, SHU-YAN QI, YAN LI, YUAN ZHAO и JI-WEI LI

School of Material Science and Engineering, Harbin University of Science and Technology, Harbin, 150040, P. R. China

Изучавана је кинетика и оптимизација обезбојавања активне комерцијалне боје argazol blue BFBR (ABB) хетерогеном Фентонском реакцијом катализованом природним шорлом. Изучавање кинетике открило је да је кинетички модел првог реда бољи за описивање обезбојавања ABB при различитим условима реакције, него модел другог реда и Behnajady–Modirshahla– Ghanbery модели. Однос између константе брзине реакције k и температуре T понашао се у складу са Аренијусовом релацијом, са привидном енергијом активације E_a од 51,31 kJ mol^{-1}. За дизајн експеримента и оптимизацију процеса обезбојавања ABB употребљен је дизајн са централним композитом по методологији површине одговора. Значај полиномијалног модела другог реда за предвиђање оптималних вредности за обезбојавање АББ оцењен је анализом варијансе и графицима 3D површина за интеракције између две променљиве. Затим су одређени оптимални услови.

(Примљено 25. фебруара 2012, ревидирано 17. јуна 2013)

REFERENCES

1. A. V. Patil, J. P. Jadhav, *Chemosphere* **92** (2013) 225
2. H. Xu, Y. Zhang, Q. Jiang, N. Reddy, Y. Yang, *J. Environ. Manage.* **125** (2013) 33

3. F. Zhang, Z. S. Zhao, R. Q. Tan, Y. Q. Guo, L. J. Cao, L. Chen, J. Li, W. Xu, Y. Yang, W. J. Song, *J. Colloid Interface Sci.* **386** (2012) 277
4. A. F. M. Alkarkhi, H. K. Lim, Y. Yusup, T. T. Teng, M. A. A. Bakar, K. S. Cheah. *J. Environ. Manage.* **122** (2013) 121
5. V. K. Gupta, R. Jain, T. A. Saleh, A. Nayak, S. Malathi, S. Agarwal. *Sep. Sci. Technol.* **46** (2011) 839
6. M. Bayat, M. Sohrabi, S. J. Royaee, *J. Ind. Eng. Chem.* **18** (2012) 957
7. S. Garcia-Segura, J. A. Garrido, R. M. Rodríguez, P. L. Cabot, F. Centellas, C. Arias, E. Brillas, *Water Res.* **46** (2012) 2067
8. M. Aleksić, H. Kušić, N. Koprivanac, D. Leszczynska, A. L. Božić, *Desalination* **257** (2010) 22
9. R. Prucek, M. Hermanek, R. Zbořil, *Appl. Catal., A* **366** (2009) 325
10. M. M. Abdel Daiem, J. Rivera-Utrilla, R. Ocampo-Pérez, J. D. Méndez-Díaz, M. Sánchez-Polo, *J. Environ. Manage.* **109** (2012) 164
11. G. Zhang, Y. Gao, Y. Zhang, Y. Guo, *Environ. Sci. Technol.* **14** (2010) 6384
12. M. Hartmann, S. Kullmann, H. Keller, *J. Mater. Chem.* **20** (2010) 9002
13. N. Dulova, M. Trapido, A. Dulov, *Environ. Technol.* **32** (2011) 439
14. Y. P. Zhao, J. Y. Hu, *Appl. Catal., B* **78** (2008) 250
15. M. Muruganandham, J. S. Yang, J. J. Wu, *Ind. Eng. Chem. Res.* **46** (2007) 691
16. W. P. Kwan, B. M. Voelker, *Environ. Sci. Technol.* **38** (2004) 3425
17. C. M. Sánchez-Sánchez, E. Expósito, J. Casado, V. Montiel, *Electrochem. Commun.* **9** (2007) 19
18. R. J. Barton, *Acta Crystallogr., B* **25** (1969) 1524
19. F. Yavuza, A. H. Gültekin, M. C. Karakaya, *Comput. Geosci.* **28** (2002) 1017
20. K. Krambrock, M. V. B. Pinheiro, S. M. Medeiros, K. J. Guedes, S. Schweizer, J.-M. Spaeth, *Nucl. Instrum. Methods, B* **191** (2002) 241
21. P. S. R. Prasad, S. D. Srinivasa, *Gondwana Res.* **8** (2005) 265
22. T. Nakamura, T. Kubo, *Ferroelectrics* **137** (1992) 13
23. H.-Y. Xu, M. Prasad, P. Wang, *Bull. Kor. Chem. Soc.* **31** (2010) 803
24. H. Xu, M. Prasad, S. Qi, Y. Li, *Sci. China Technol. Sci.* **53** (2010) 3014
25. H.-Y. Xu, M. Prasad, Y. Liu, *J. Hazard. Mater.* **165** (2009) 1186
26. S. Tunç, T. Gürkan, O. Duman, *Chem. Eng. J.* **181**–**182** (2012) 431
27. S. Karthikeyan, V. K. Gupta, R. Boopathy, A. Titus, G. Sekaran, *J. Mol. Liq.* **173** (2012) 153
28. İ. Gulkaya, G. A. Surucu, F. B. Dilek, *J. Hazard. Mater.* **136** (2006) 763
29. M. Fathinia, A. R. Khataee, M. Zarei, S. Aber, *J. Mol. Catal., A* **333** (2010) 73
30. A. R. Khataee, M. Safarpour, M. Zarei, S. Aber, *J. Mol. Catal., A* **363**–**364** (2012) 58
31. M. G. Lak, M. R. Sabour, A. Amiri, O. Rabbani, *Waste Manage.* **32** (2012) 1895
32. E. Rosales, M. A. Sanromán, M. Pazos, *Environ. Sci. Pollut. Res.* **19** (2012) 1738
33. R. Idel-aouad, M. Valiente, A. Yaacoubi, B. Tanouti, M. López-Mesas, *J. Hazard. Mater.* **186** (2011) 745
34. W. P. Kwan, B. M. Voelker, *Environ. Sci. Technol.* **37** (2003) 1150
35. H. Che, S. Bae, W. Lee, *J. Hazard. Mater.* **185** (2011) 1355
36. R. Andreozzi, V. Caprio, R. Marotta, *Water Res.* **36** (2002) 2761
37. J. Feng, X. Hu, P. L. Yue, *Environ. Sci. Technol.* **38** (2004) 269
38. H. Wu, X. Dou, D. Deng, Y. Guan, L. Zhang, G. He, *Environ. Technol.* **33** (2012) 1545
39. X. Liang, Y. Zhong, S. Zhu, J. Zhu, P. Yuan, H. He, J. Zhang, *J. Hazard. Mater.* **181** (2010) 112

40. M. Karatas, Y. A. Argun, M. E. Argun. *J. Ind. Eng. Chem.* **18** (2012) 1058
41. M. Azami, M. Bahram, S. Nouri, A. Naseri, *J. Serb. Chem. Soc*. **77** (2012) 235
42. S.-P. Sun, A. T. Lemley, *J. Mol. Catal., A* **349** (2011) 71
43. S. Mohajeri, H. A. Aziz, M. H. Isa, M. A. Zahed, M. N. Adlan, *J. Hazard. Mater*. **176** (2010) 749.